

N72-23A2

HEAT TRANSFER AND THERMAL STRATIFICATION IN THE
APOLLO 14 CRYOGENIC OXYGEN TANKS

By

S. S. Fineblum, A. S. Haron, J. A. Saxton
Bellcomm
Washington, D. C.

INTRODUCTION

Two significant facets of Apollo oxygen tank operation are the occurrence of thermal stratification at high fluid densities and the tendency toward high heater temperatures at low fluid densities. Some insight into the nature of these phenomena can be gained, respectively, by consideration of a two fluid stratification model and a conductive heat transfer model. The alternative of convective blowdown tank operation at low densities is briefly examined.

STRATIFICATION

Thermal stratification is significant in the Apollo oxygen tanks because of the greatly reduced mixing in the low gravity field and the low thermal conductivity of the oxygen. In the stratified tank adjacent phases of different temperature coexist stably. The less dense phase exerts a pressurizing influence on the relatively incompressible dense phase. The effects of stratification are for the most part limited to high density conditions; for example, pressure decays have not been observed on Apollo flights for densities of less than $\sim 42 \text{ lb/ft}^3$ (60% tank quantity). The phenomena of pressure decay relates to the fact that at the higher densities the energy input necessary to achieve a given pressure rise is measurably less with stratification than without. Hence the tank can maintain operating pressure despite a small energy deficit;

induced mixing, as caused by a vehicle maneuver, then results in a sudden pressure drop or decay.

By conservation of energy the relation between energy input, mass outflow, and pressure rise rate for a homogeneous fluid is:

$$\frac{dp}{dt} = \frac{C\phi}{V} (Q - \omega\theta) \quad (1)$$

where

$$\phi \equiv \frac{1}{\rho} \left(\frac{\partial p}{\partial u} \right)_{\rho} \quad (2)$$

$$\theta \equiv -\rho \left(\frac{\partial h}{\partial p} \right)_{p} \quad (3)$$

$$C = \left(1 + \frac{\rho\theta\phi}{V} \frac{dV}{dp} \right)^{-1} \quad (4)$$

and Q , ω , V , p , u , and h are the heat input, mass outflow, volume, pressure, internal energy, and enthalpy, respectively. The coefficient C accounts for the change in tank volume with increasing pressure. Equations (1) - (4) yield the pressure rise rate when heat is added uniformly, that is, stratification does not occur.

Over the entire pressure cycle the energy input is related solely to the fluid's enthalpy-density relationship θ and the rate of mass outflow from the tank ω . That is, there is no net pressure change so Equation (1) becomes

$$Q = \omega\theta \quad (5)$$

Figure 1 shows the energy input data for Apollo 14. The solid curves were computed by Equation (5) for a mean tank pressure of 900 psi using the average flow rates and heat

leaks indicated. Tank quantity rather than density is used as the abscissa, with 100% quantity equal to 69.5 lb/ft³. The spread in the data reflects the variation of the flow rates about the mean value.

The time to pressurize the tank within its operating band offers a direct measure of the stratification occurring. Figure 2 portrays this data for Apollos 12 and 14. The spread of the data points below 60% for the two missions is traceable to two effects.* Firstly, because of the tank arrangement on Apollo 14, Tank 3 mass outflow during its heater operation was substantially increased by leakage of the Tank 2 check valve. In effect Tank 3 pressurized Tank 2 during each cycle. Secondly, for thermal reasons only two of the three Tank 3 heater elements were employed below 41% (with two exceptions). With this in mind the pressurization times for Apollos 12 and 14 are essentially identical even though Apollo 12 utilized fans for periodic mixing (twice daily). That is, the fan operations did not appear to noticeably reduce stratification effects on pressurization.

In Figure 3 the Apollo 14 data are plotted with the pressurization time predicted by Equations (1) - (4) indicated by the solid lines. The flowrates employed are given in Figure 4. The flow values are taken from the quantity guage readings, corrected in the case of Tank 3 for the flow necessary to pressurize Tank 2. As expected, the agreement between data and prediction is relatively good below 60%, but not above.

*Note: On Apollo 14 all data above 60% is from Tanks 1 and 2 and below 60% is from Tank 3; whereas on Apollo 12 Tanks 1 and 2 were operated concurrently throughout (there was no third tank).

The basic elements of the effect of stratification on pressurization are the localized storage of energy in the vicinity of the heater and the nature of the enthalpy-density relationship as reflected in θ . Following heater activation the fluid adjacent to the heater increases in temperature, and hence expands. This expansion mechanically pressurizes the remainder of the fluid. The pressurization of the bulk fluid by the hot "bubble" is given by

$$\Delta p = \left(\frac{\partial p}{\partial h}\right)_{\rho} \Delta h + \left(\frac{\partial p}{\partial \rho}\right)_h \Delta \rho = - \left(\frac{c \rho \phi \theta}{V}\right)_B \Delta V_B \quad (6)$$

where the tank heat leak and outflow have been neglected. The bulk's volume change is equal and opposite to that of the bubble, whose mass is assumed constant:

$$\Delta V_B = -\Delta V_s = \left(\frac{V}{\rho \phi \theta}\right)_s \Delta \rho - \left(\frac{1}{\rho \theta}\right)_s \Delta Q \quad (7)$$

The stratified pressure response of the system, Δp , to a localized heat input, ΔQ , is therefore given by:

$$\Delta p = \frac{\frac{\rho_B \theta_B}{\rho_s \theta_s} \frac{C \phi_B}{V_B} \Delta Q}{1 + \frac{\rho_B \theta_B \phi_B}{\rho_s \theta_s \phi_s} \frac{V_s}{V_B} C} \quad (8)$$

with subscripts s and B referring to the stratified bubble and bulk fluid, respectively. The θ curve passes through a minimum at a density of $\sim 26 \text{ lb/ft}^3$. If the bulk density is greater than this, the θ and ρ variations accompanying the creation of a less dense phase (film) adjacent to the heater combine to cause a larger pressure rise for a given

heat input. Below $\sim 42 \text{ lb/ft}^3$ density (60%) the θ decrease with expansion falls off and below 26 lb/ft^3 the θ variation counteracts the effect of density decrease on pressure rise.

A rough indication of the extent of the stratification process can be gained by a two fluid calculation. The model is schematically depicted in Figure 5. Initially all heater energy Q_{HTR} is assumed confined to the stratified volume adjacent to the heater. The energy is accommodated by fluid outflow m_1 from this volume. The bulk fluid receives this stratified outflow as well as heat leak Q_{HLK} from the environment and supplies tank outflow m_0 to the spacecraft systems. Equations (1) - (4) describe the pressure rise in each phase. When the stratified fluid density has diminished to that point where its θ value has passed through the minimum and risen to the bulk value, the heater energy is assumed to be transferred uniformly to the bulk phase. Of course, other phenomena take place, such as stratified volume growth, mass transfer from the bulk, and energy sharing with the bulk. Nevertheless, the simplified model exhibits the basic attributes of the observed pressure behavior as shown by the dashed line in Figure 3. The calculation results are for a stratified volume of 0.0119 ft^3 (1/4% of tank volume) or a radial distance of 1/8 inch. This is on the order of boundary layer dimensions, and explains the insensitivity of pressurization times to overall tank flow condition as evidenced by the close grouping of Apollo 12 and 14 data for a variety of spacecraft inertial conditions.

Some interesting aspects of stratification are shown in Figure 6. Here fan activation causes the expected pressure decay. The divergence from uniform heating conditions of the pressure profile prior to fan operation reflects stratification. The pressure behavior during the heater cycle following fan operation is significant, though. As expected, in the well mixed tank the pressure behavior follows a uniform heating path. However, the recovery from the low pressure point occurs at a rate identical to the pressure rise rate prior to fan operation. Hence, even in this clearly active fluid motion environment some stratification of the same type as that observed in the quiescent period prior to fan operation occurs.

CONDUCTIVE HEAT TRANSFER MODEL

Since the gravitational forces exerted on the vehicle during steady flight are quite small, ranging from roughly $7 \times 10^{-8}g$ in attitude hold to $3 \times 10^{-6}g$ during 3 rph passive thermal control, the buoyant motion of the fluid during heat transfer periods is correspondingly reduced. In the limit, heat is transferred into the fluid solely by conduction. This constitutes a worst case in terms of maintaining a low heater temperature while transferring the heat required to sustain tank operating pressure. Therefore, a conduction model was developed to predict worst case (zero gravity) heater temperatures (Reference 1).

The simplified model is schematically depicted in Figure 7. It assumes spherical symmetry (as the tank) and adapts the cylindrical heater parameters to this configuration. The spherical heater area is set equal to its cylindrical counterpart, while its internal volume is adjusted to match the true cylindrical volume. Twelve fluid nodes of equal thickness are dispersed between the heater and tank wall; the fluid within the heater is represented by one node; and the heater, tank wall and SM environment are represented by one node each.

The CINDA-3G numerical heat transfer program was employed. The logic of this program is shown in Figure 8 via its electrical analogue where each node with its own capacitance is linked to adjacent nodes by resistive circuits. The radiative transfer between the heater and the tank wall is included as is the heat leak to the tank from the surrounding environment. Tank pressure is held constant throughout each calculation, and the nodal mass, specific heat, and thermal conductivity are adjusted at each time step in accord with the nodal temperatures resulting from the conductive heat transfer. The oxygen properties as correlated by R. B. Stewart (Reference 2) are employed for density and specific heat, while the thermal conductivity is taken from a North American Rockwell report (Reference 3).

The model is admittedly crude. It does, however, furnish some interesting results. Firstly, the predicted

temperatures agree well with those for steady attitude hold heater cycles. Figure 9 illustrates this. Here the temperature profile and maximum temperature indicated by the heater temperature sensor are closely matched by the model. (One qualification to be made is that the model assumes a uniform heater temperature while the data is from a thermocouple linked to one point on the heater. The excellent correlation between the two is taken to mean that the temperature sensor reflects an effective mean heater temperature from a heat transfer standpoint.) It appears that some mixing occurred at the beginning of the heating cycle but after this delay the temperature rise and fall off after heater deactivation are as predicted. Thus, the g forces exerted during attitude hold seem to produce little convective mixing, although the more rapid return of the heater to its original temperature indicates some convection.

It is interesting to look next at the ability of spacecraft rotation to enhance heat transfer. Figures 10 and 11 show the heater temperature profiles for rotation rates of 1 rph and 3 rph respectively. The ratio of the maximum temperature rise achieved in each case to the maximum temperature rise predicted by the conductive model offers a rough measure of the convective heat transfer coefficient. The increased rate of rotation clearly produces improved heat transfer.

Another form of convective motion is shown in Figure 12. Here the spacecraft has been brought to rest from a 3 rph passive thermal control rotation. The low temperatures indicate substantial fluid motion. By comparison, Figure 9 for attitude hold eight hours after the cessation of 1 rph rotation shows little evidence of fluid motion.

From the foregoing we conclude that a simplified conductive model closely models attitude hold conditions and can serve as a useful real time indicator of the level of convective motion in the tanks.

CONVECTIVE BLOWDOWN

The energy input required to maintain tank operating pressures of 900 psi increases sharply as low tank quantities are approached, and the dilute gas offers a diminished energy sink for the heater. Thus high heater temperatures may be encountered. An alternative operational mode is to take advantage of the pressurization energy and operate the tank as a compressed gas source. A constraint is that tank pressure be maintained at greater than 150 psi for proper flow to the fuel cells. One way of satisfying this requirement is to add sufficient energy to follow an isothermal path once past the apex of the two phase region, for example the -160° F isotherm in Figure 13. The energy required for total evacuation from 20% (71.3 lb) via such an isothermal blowdown is given in Figure 14 as a function of tank outflow rate. A portion of the needed heat is provided by heat leak from the surrounding environment. In fact, the heat leak supplies all necessary energy for evacuation at an outflow rate of 0.5 lb/hr, and the heater duty cycles for 1.0 and 1.5 lb/hr flows are minimal (<10%).

CONCLUSIONS

Two simplified models have been found to yield useful insights into the oxygen tank thermal behavior. The two fluid stratification model indicates that stratification of less than 1% of the fluid will lead to the observed pressure response times. The involvement of such a small fluid volume explains the insensitivity of the pressurization times to overall tank fluid motion and the rapid pressure recovery following fan operation. The conductive/radiative heat transfer model furnishes a worst case heater temperature prediction and can serve as an indication of the extent of convective mixing. It is seen that the g-force exerted during attitude hold is insignificant in terms of enhanced heat transfer, but that ~ 3 rph passive thermal control has a noticeable effect.

ACKNOWLEDGMENT

The significant contribution of M. V. Drickman in adapting R. B. Stewart's programs for the thermodynamic properties of oxygen to the Bellcomm computer and developing a number of related subprograms is gratefully acknowledged.

REFERENCES

1. Haron, A. S., "Transient Analysis of Heat Transfer in a Simplified Model of the Apollo Oxygen Tank", Bellcomm Memorandum for File, B70 12076, December 30, 1970.
2. Stewart, R. B., "The Thermodynamic Properties of Oxygen", PhD Thesis, University of Iowa, 1966.
3. Moses, R. E., "Internal Communication", Rocketdyne, Space Division of North American Rockwell, Inc., April 1964.

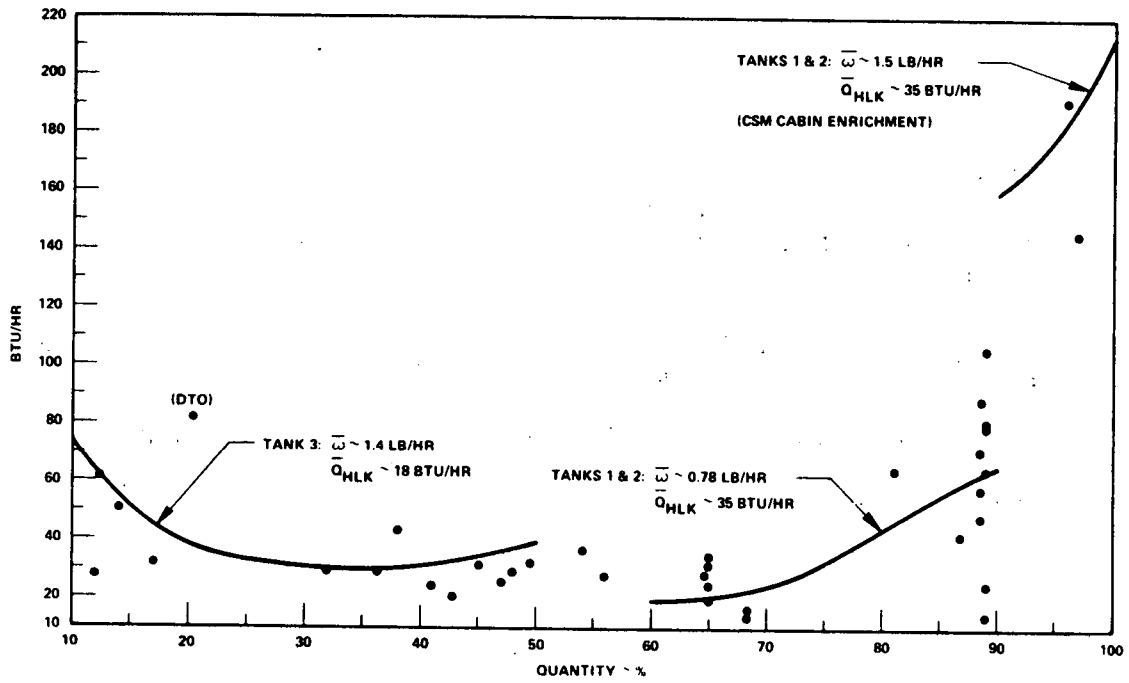


FIGURE 1 - ENERGY INPUT RATE AS FUNCTION OF QUANTITY AND FLOW RATE

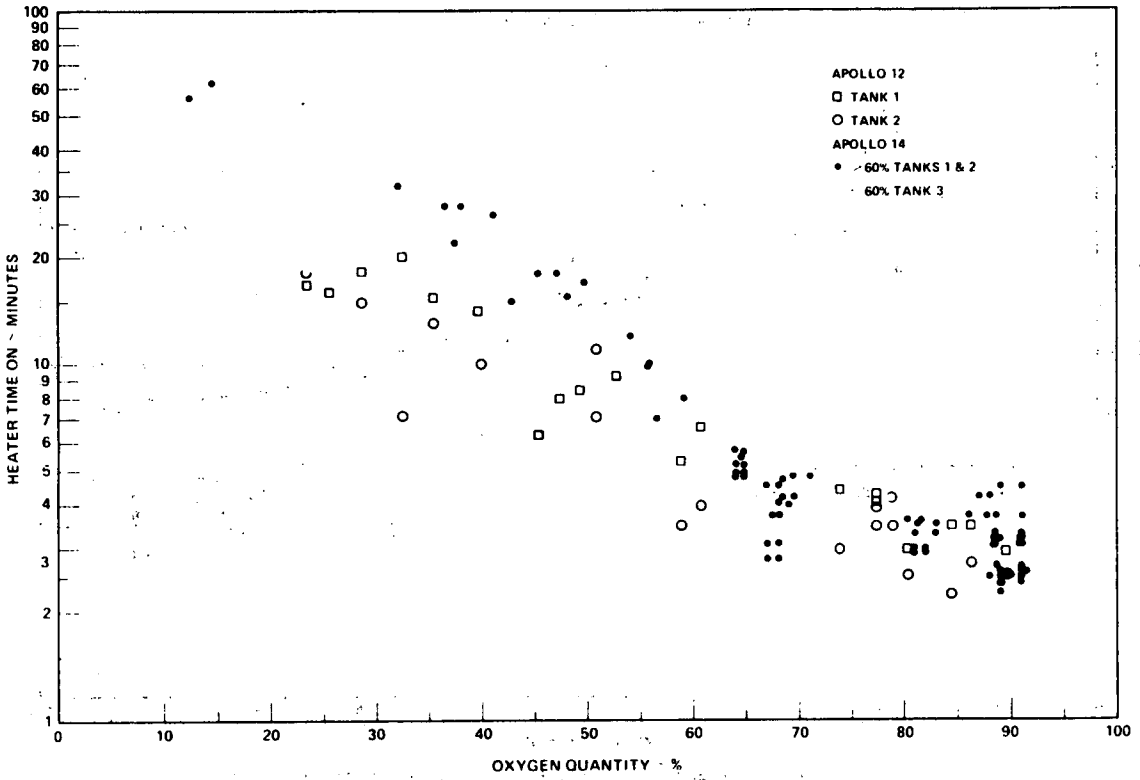


FIGURE 2 APOLLOS 12/14 PRESSURIZATION TIMES

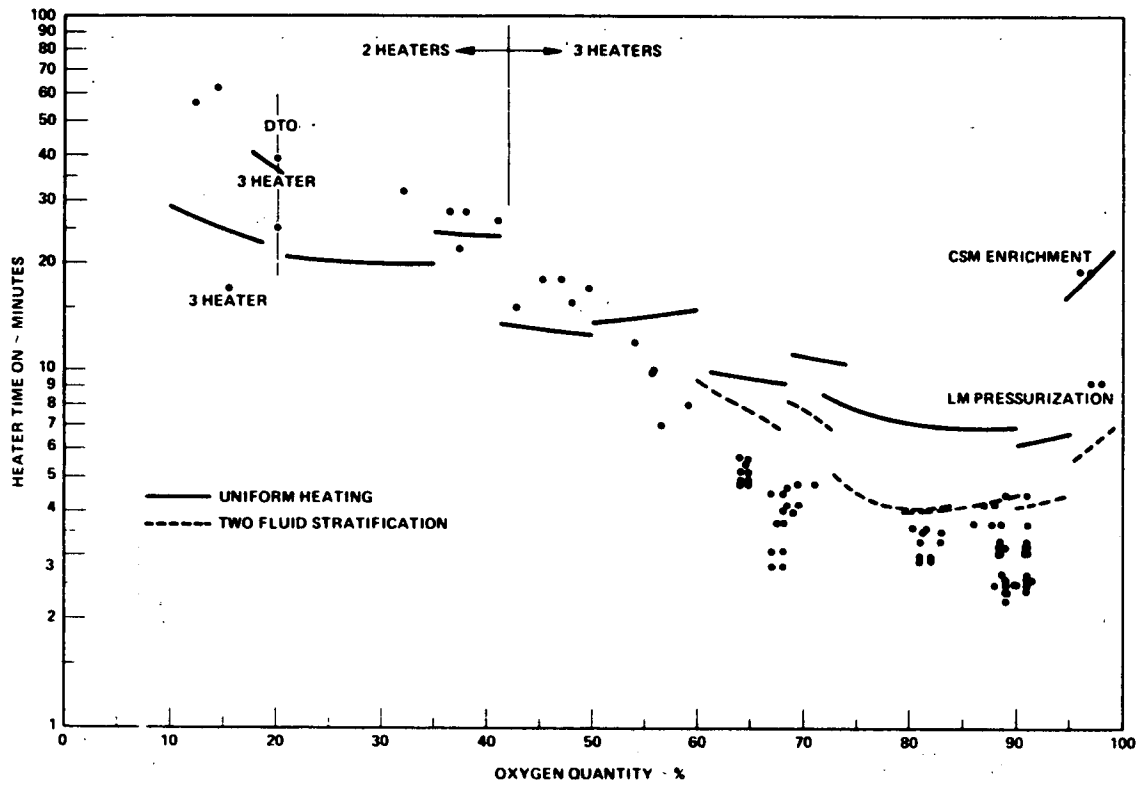


FIGURE 3 APOLLO 14 PRESSURIZATION TIMES DEPICTING EFFECT OF STRATIFICATION

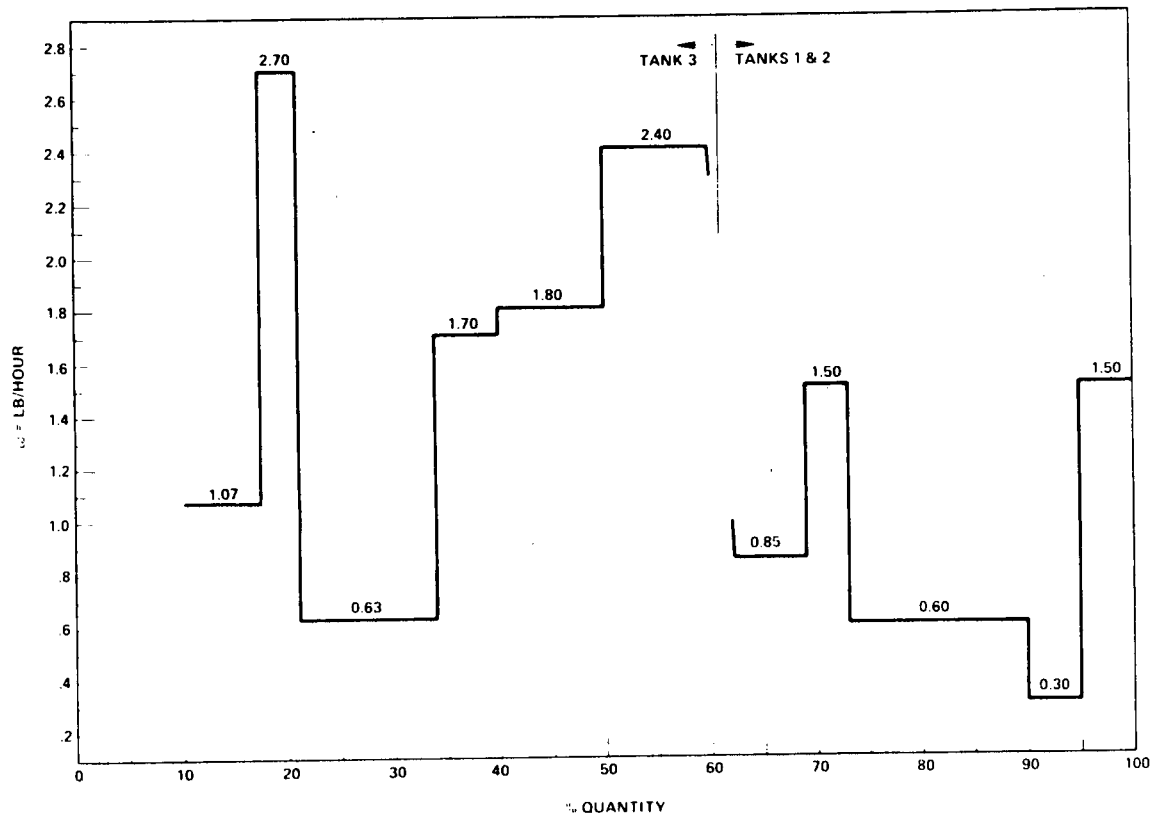


FIGURE 4 APOLLO 14 AVERAGE O₂ FLOW RATES DURING HEATING OPERATION

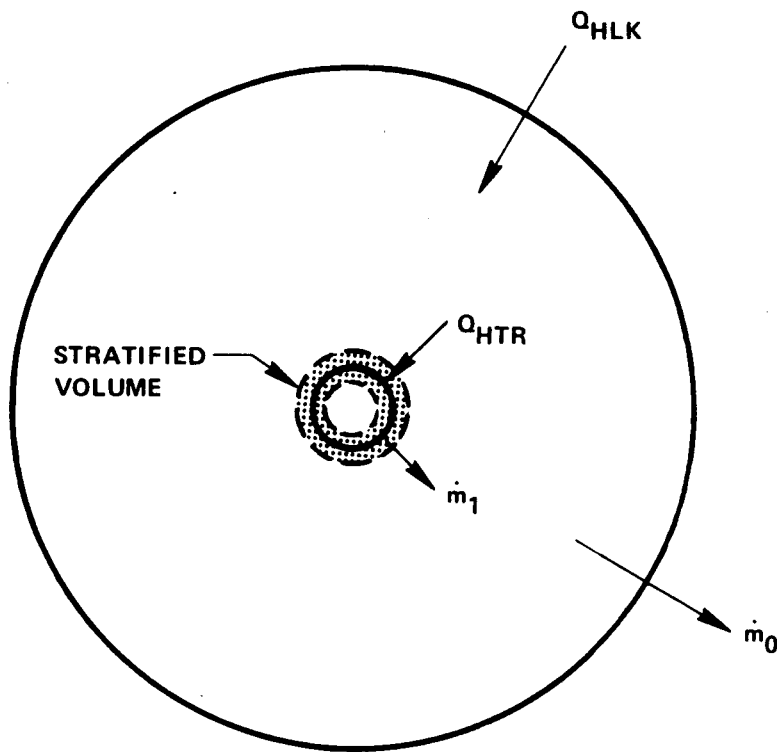


FIGURE 5 - SCHEMATIC OF TWO FLUID MODEL

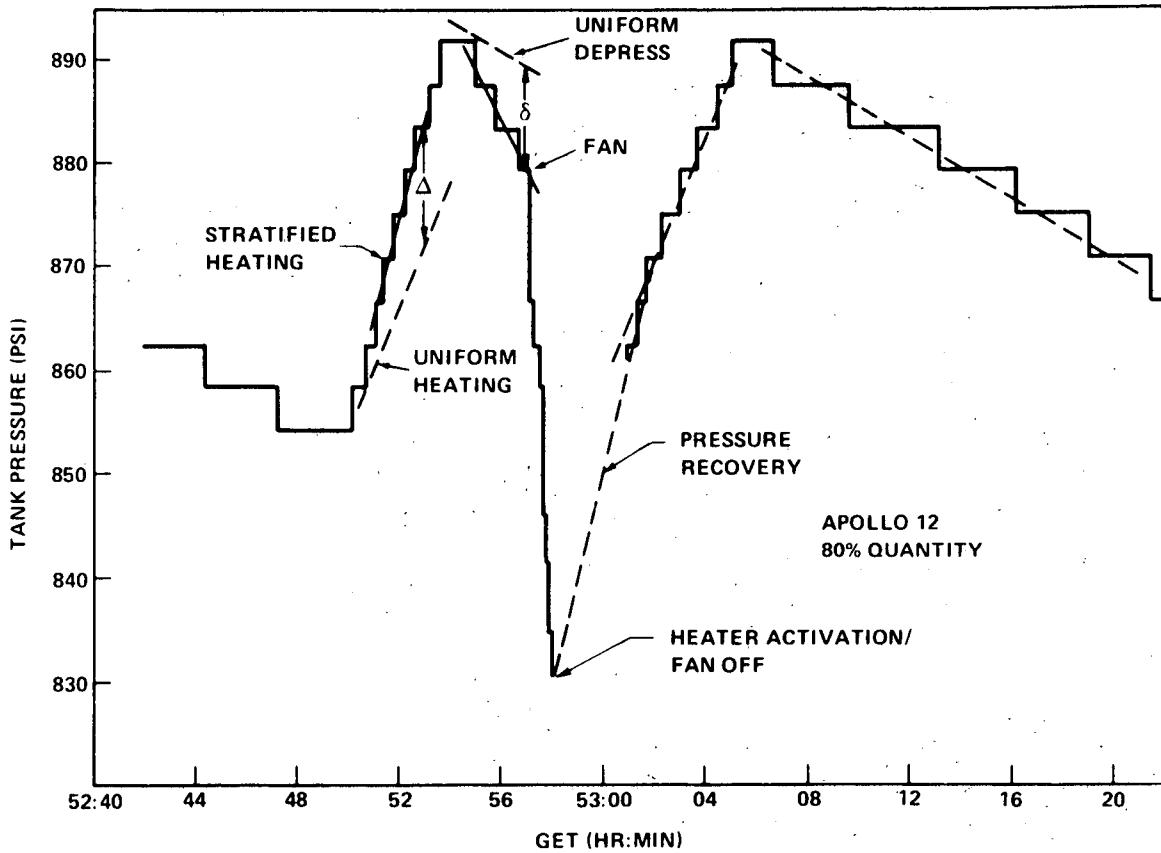
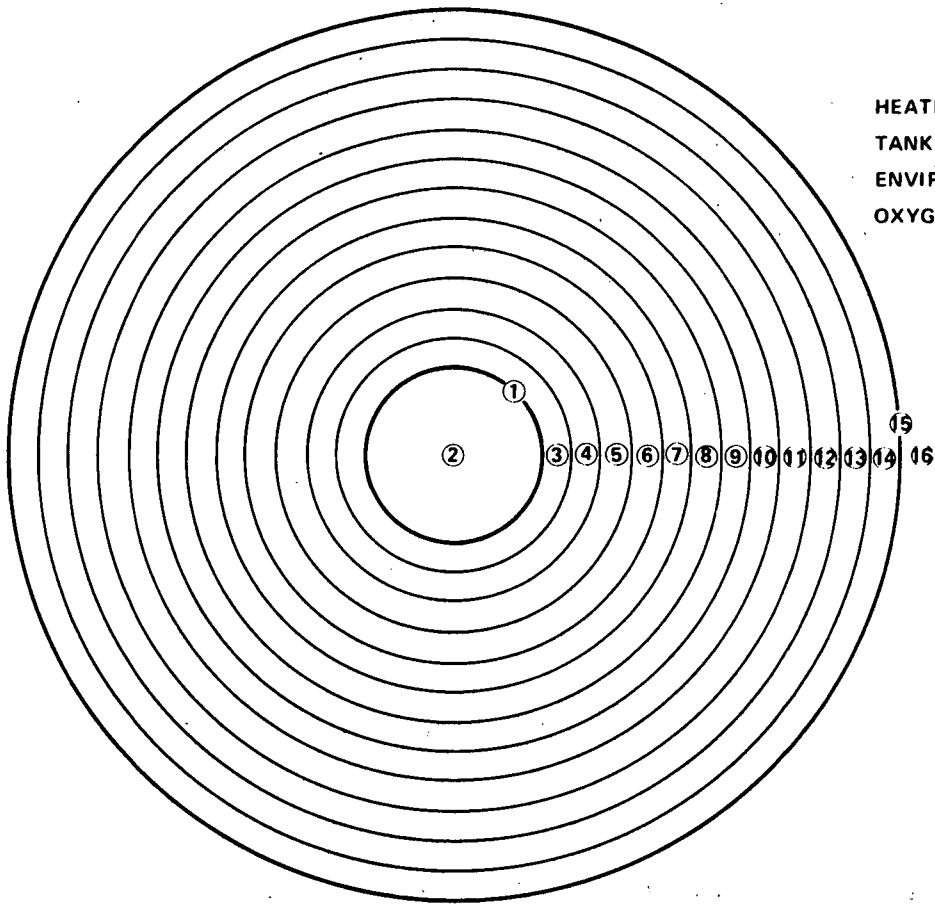
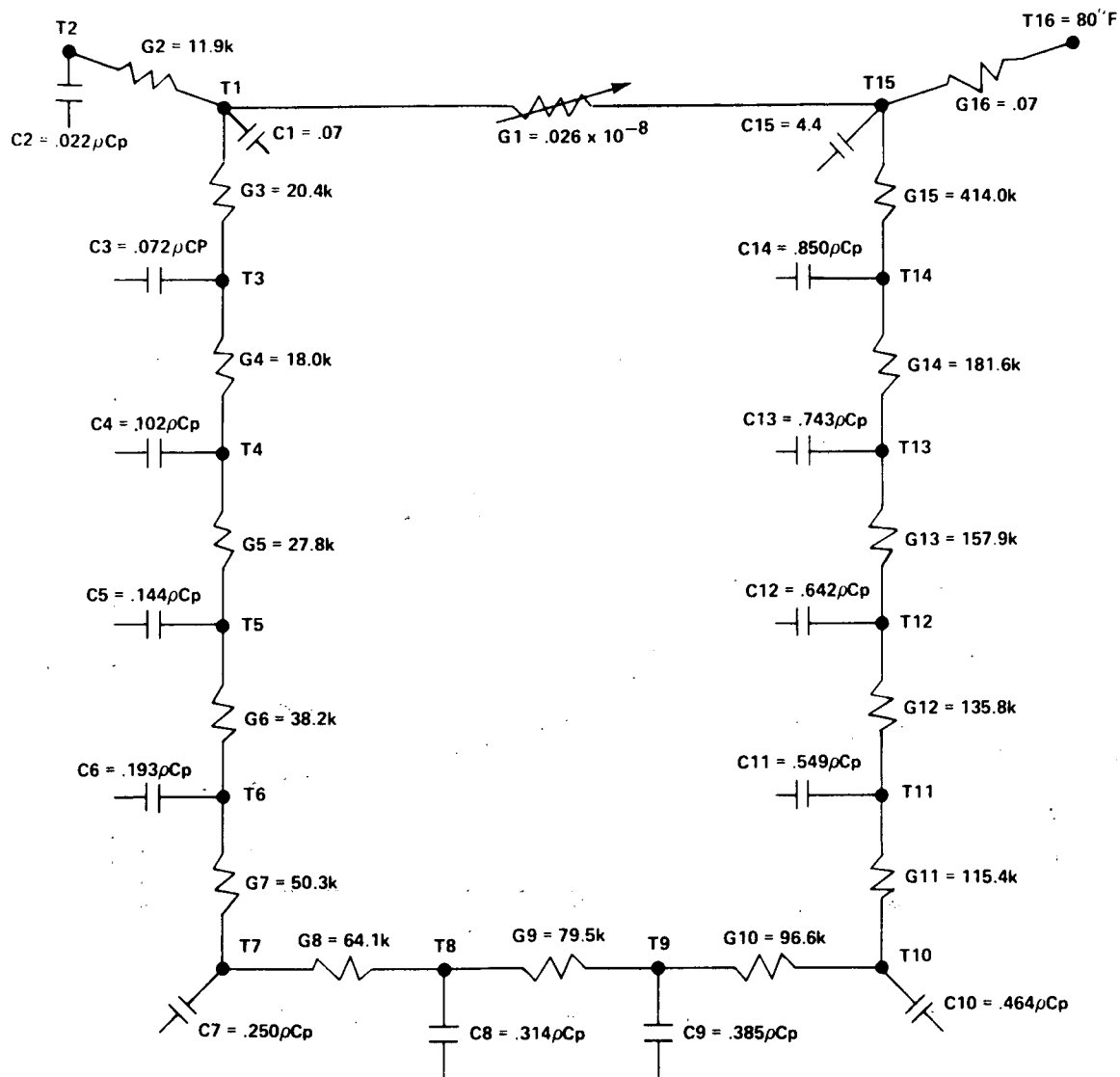


FIGURE 6 - PRESSURE CYCLES BEFORE/AFTER FAN CYCLE



HEATER: NODE # 1
TANK WALL: NODE # 15
ENVIRONMENT: NODE # 16
OXYGEN: NODES # 2 - 14

FIGURE 7 - OXYGEN TANK PHYSICAL MODEL



TX = TEMPERATURE OF NODE "X"
 CX = MASS X SPECIFIC HEAT OF NODE "X" IN BTU/°F \equiv (VOLUME) (ρ Cp)
 GX = EFFECTIVE CONDUCTANCE BETWEEN ADJACENT NODES IN BTU/HR °F \equiv kA/ χ
 G1 = EFFECTIVE RADIANCE BETWEEN NODES (1) AND (15) IN BTU/HR °F⁴ \equiv A ϵ σ

FIGURE 8 - NETWORK DIAGRAM OF OXYGEN TANK THERMAL MODEL

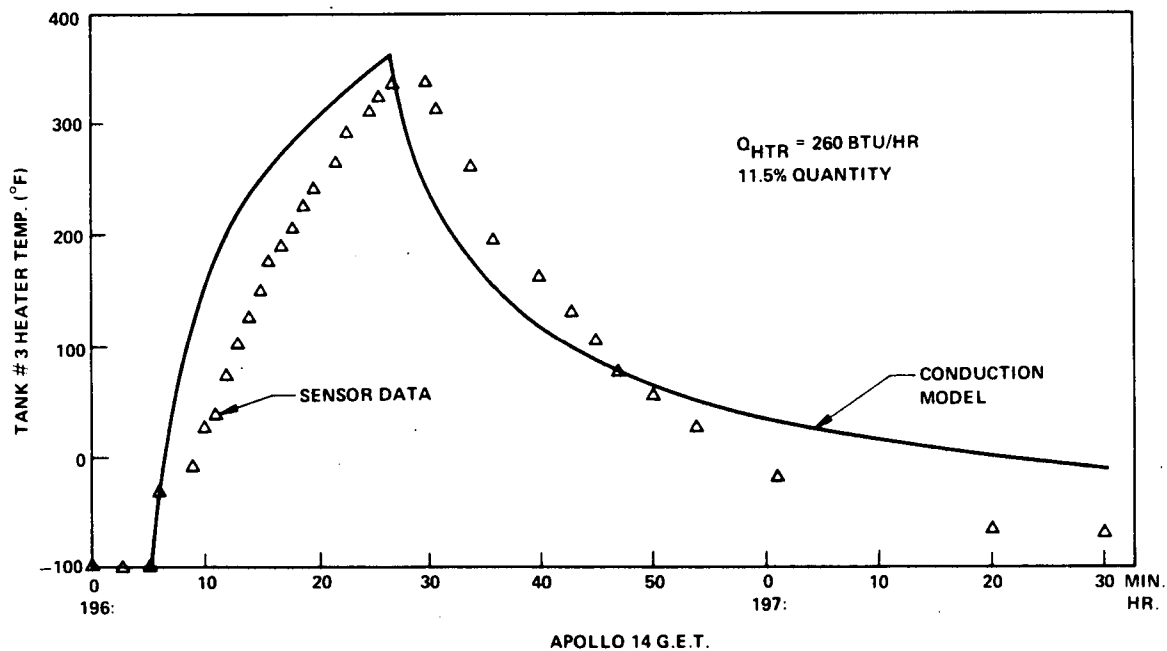


FIGURE 9 - HEATER TEMPERATURE PROFILE DURING ATTITUDE HOLD

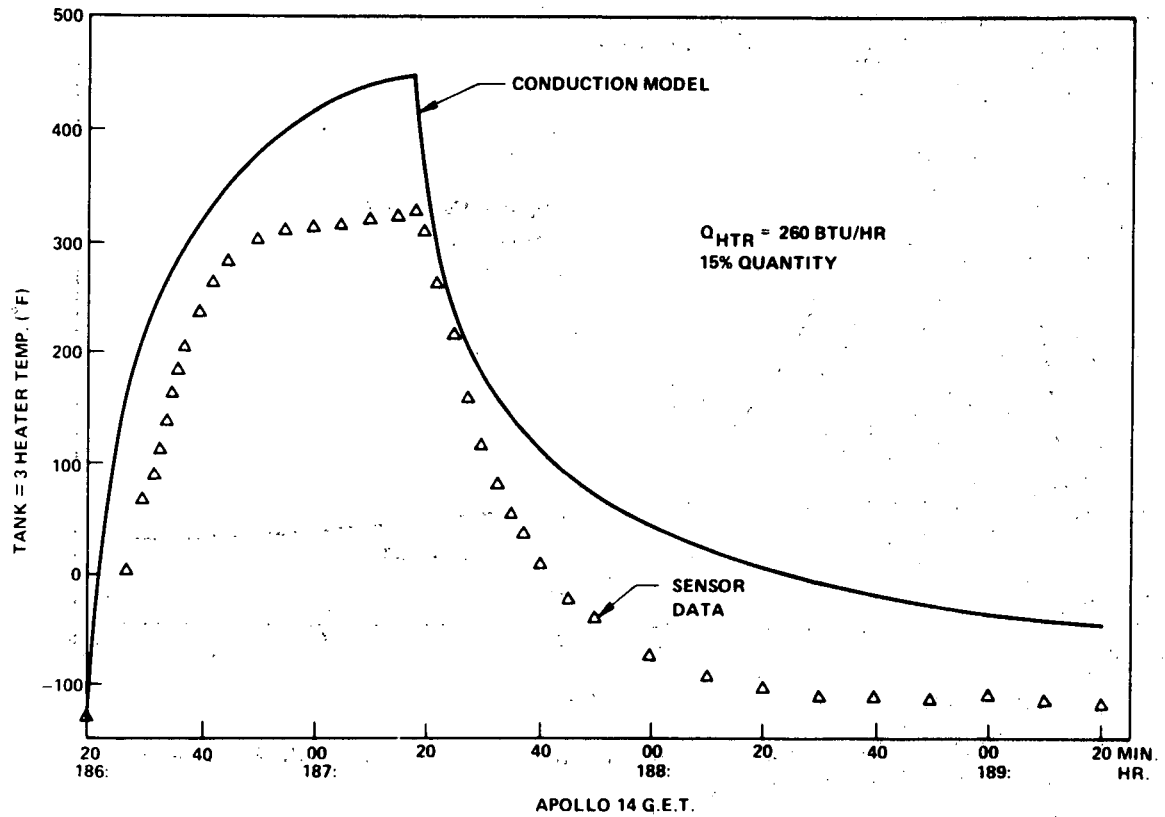


FIGURE 10 - HEATER TEMPERATURE PROFILE DURING 1 RPH SPACECRAFT ROTATION

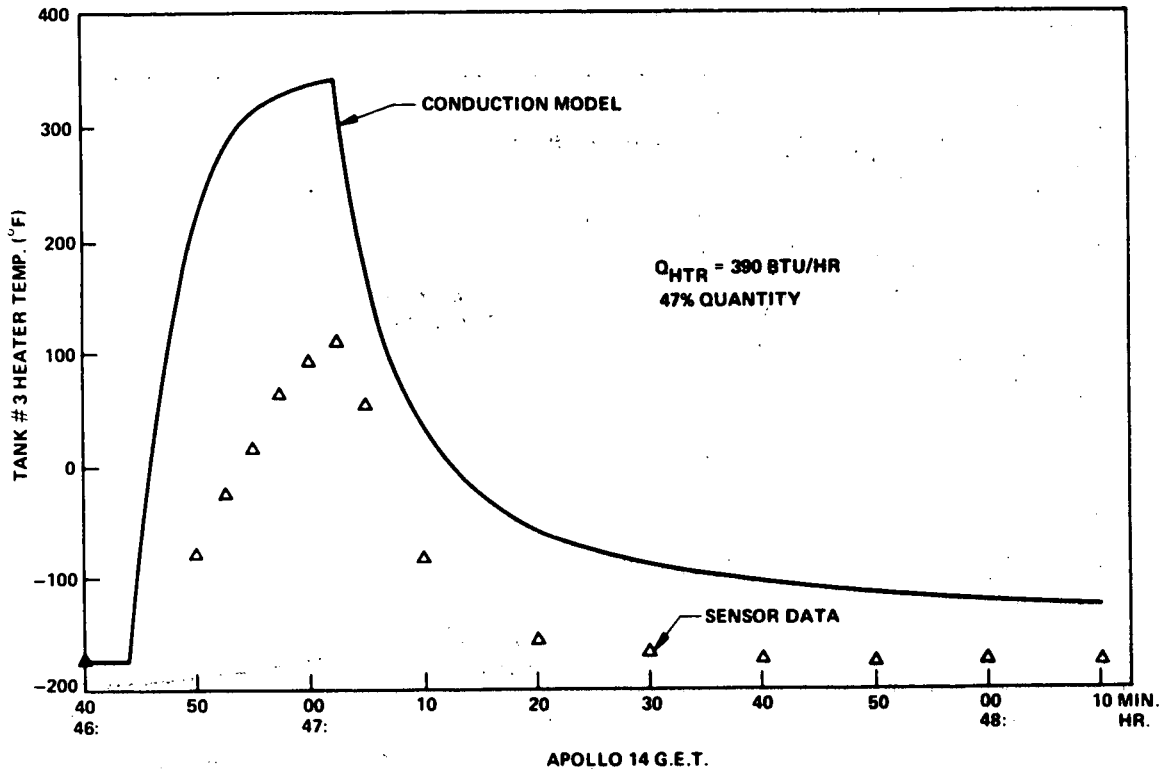


FIGURE 11 - HEATER TEMPERATURE PROFILE DURING ~ 3 RPH SPACECRAFT ROTATION

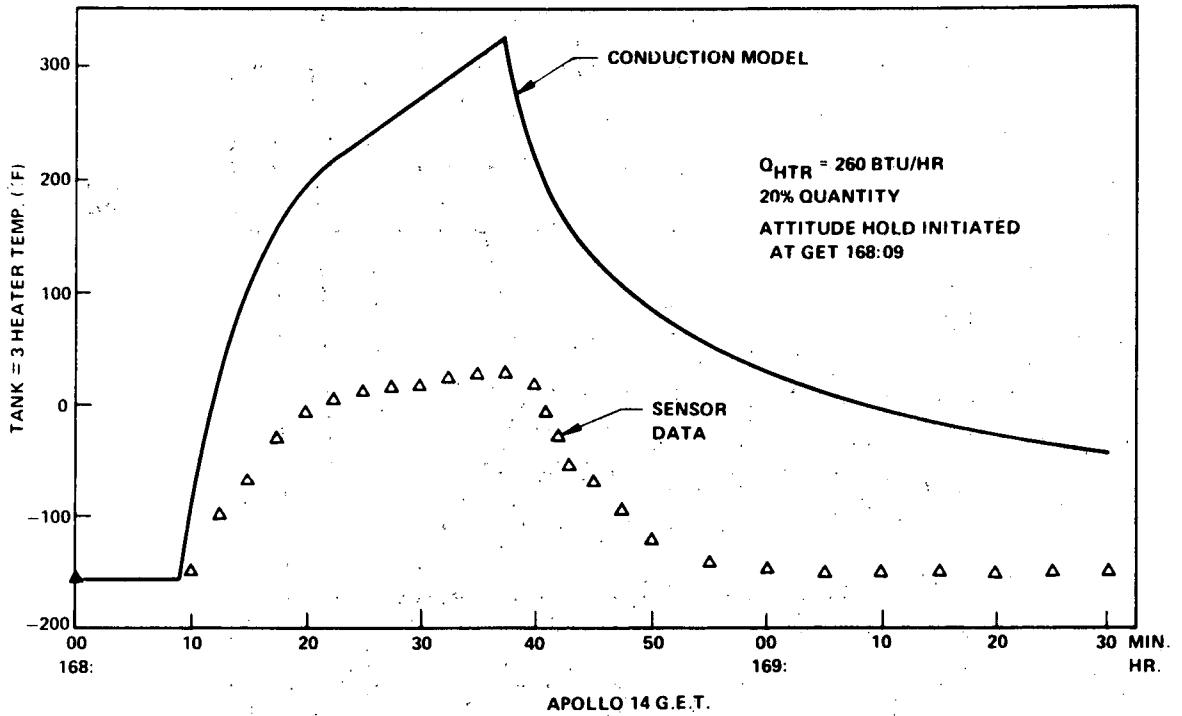


FIGURE 12 - HEATER TEMPERATURE PROFILE FOLLOWING SPACECRAFT ROTATIONAL MANEUVER

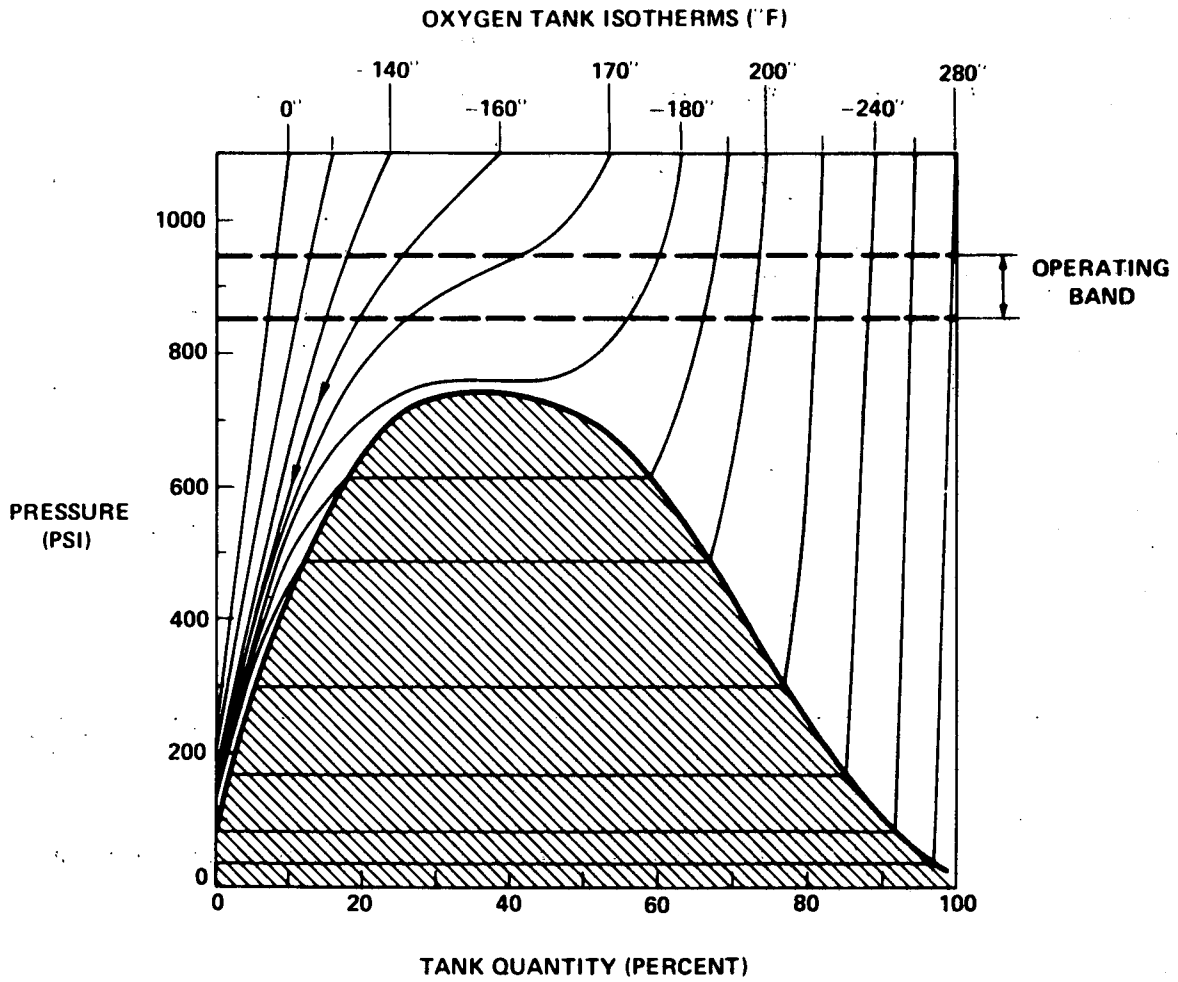


FIGURE 13 - OXYGEN SUPPLY PRESSURE VERSUS TANK QUANTITY

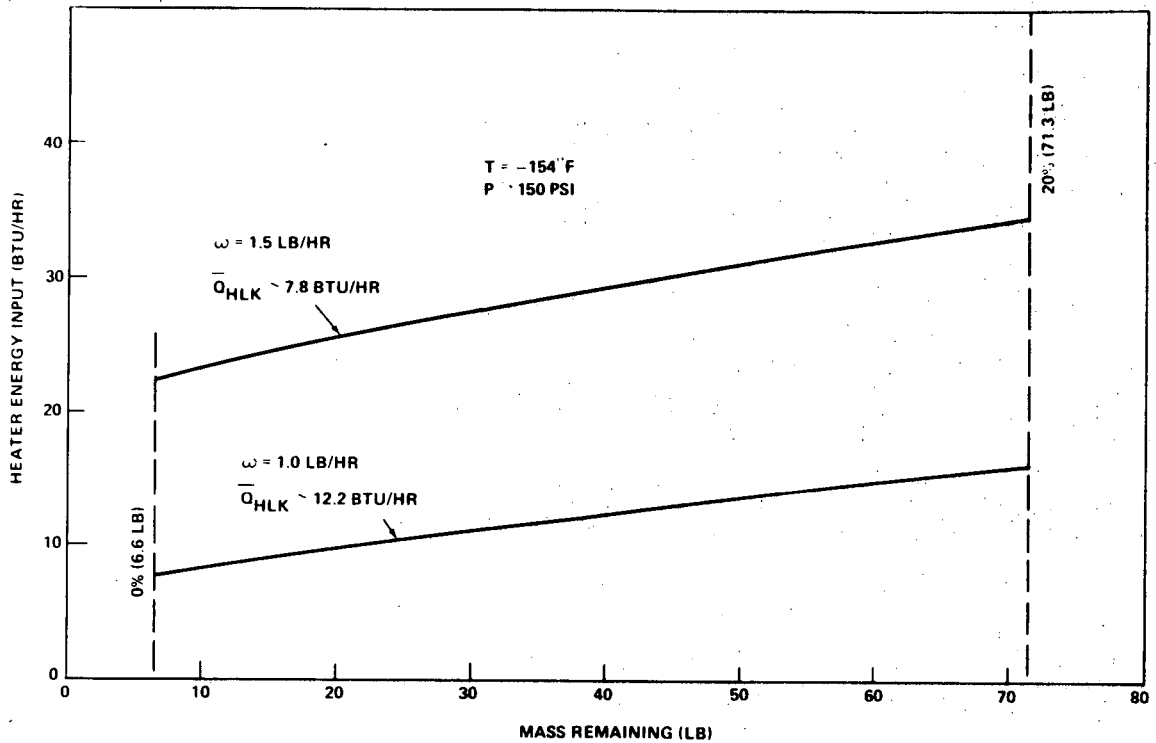


FIGURE 14 - HEATER ENERGY INPUT FOR ISOTHERMAL BLOWDOWN FROM 20% QUANTITY